Coriolis Force: Conservation Principles for Motion on the Rotating Earth

Boyd and John Edwards
(Dated: December 16, 2018)

In this paper, we determine when energy and angular momentum are conserved for motion on a spinning, frictionless, smooth earth, for both spherical and elliptical earth shapes.

I. INTRODUCTION

In 1679, Sir Isaac Newton and Robert Hooke discussed the possibility that the horizontal deflection of falling objects could serve as proof of the Earth's rotation; this possibility was confirmed in an 1803 measurement that agreed with calculations by Gauss and Laplace [1]. In 1835, Gaspard Gustave Coriolis showed that the total inertial force in a rotating frame is the sum of two forces, the centrifugal force and a "deflective force" that is now known as the Coriolis force [1, 2].

Despite its long history of study, the Coriolis force is a continuing source of difficulty, including student frustration [3], confusion over its role in bathtub vortices [4], textbook errors and omissions [5], errors in the literature [6, 7], and blunders by Richard Feynman and Max Born [8–10]. The Coriolis deflection can seem downright mysterious, as anyone who has played catch on a merry-go-round can attest [11]. Students of intermediate (upper-division) classical mechanics learn how to transform Newton's second law into a uniformly rotating frame mathematically, but they often cannot interpret the mathematics, appreciate the physical origins of the Coriolis and centrifugal forces, connect them with other theories and conservation laws, or relate them to motion as seen in the inertial frame [12, 13]. At least one popular intermediate classical mechanics treatment of the Coriolis force presents the mathematics and little else [14].

In contrast with the relatively simple two-dimensional inertial forces for motion on a rotating platform, physical insight into three-dimensional inertial forces for motion on a rotating planet is difficult to come by [15], despite its importance in meteorology [16], oceanography [17], long-range ballistics and sniping, satellite tracking, aviation, and Jovian wind patterns [18]. Challenges to understanding these inertial forces include: (a) their three-dimensionality and latitude dependence, (b) the lack of any simple physical demonstrations [15], and (c) the ellipsoidal (non-spherical) shape of the earth. The Coriolis force is key to the understanding of large-scale motions on our planet's surface, yet understanding of this force is often lacking, incomplete, or incorrect. Because the Coriolis force touches so many aspects of our planet's behavior, and plays such a key role in our history and culture, it is imperative that information about this subject be correct, clear, and insightful [5].

To explain why the Coriolis force deflects objects to the right in the northern hemisphere and to the left in the southern hemisphere, authors often rely on Hadley's principle [19, 20], which is simple, convenient, and wrong [7]. This principle is used widely in introductory earth science textbooks to explain the physical origins of the Coriolis deflection [16, 21–23]. Hadley's principle is pervasive because it correctly predicts the direction of the Coriolis deflection for north-bound and south-bound motion. But Hadley's principle suffers from fatal deficiencies: (a) it accounts for only half of the Coriolis deflection, (b) it includes only one of the two mechanisms responsible for this deflection, and (c) it violates conservation of angular momentum and conservation of energy [3].

Many authors, some of them unfamiliar with Hadley's work, treat the eastward component of velocity (as seen by the inertial observer) as a constant as an object moves northward in the northern hemisphere [21–23], or treat the eastward component of velocity (as seen by the inertial observer) to be constant as an object drops vertically [6, 24–26], a clear violation of conservation of angular momentum. The physics and meteorology literatures are riddled with such blunders, and errors and omissions abound [3, 5, 7, 8]. For both northward and vertical motion, conservation of angular momentum is needed to correctly account for Coriolis deflections [27–29].

McIntyre [15] treats the motion of a hockey puck on the surface of a uniform, spherical, frictionless "frozen" earth. In this case, the puck executes uniform circular motion in great circles around the center of the sphere, as seen by an observer in the fixed (inertial) frame, visiting both the northern and southern hemispheres equally. As seen by an earthbound observer in the rotating (non-inertial) frame, the puck is subject to two inertial forces, the Coriolis force and the centrifugal force. For the frictionless spherical earth, objects that are released from rest by this earthbound observer experience an unbalanced centrifugal force that drives them toward the equator.

The earth is not spherical, and motion on the surface of our ellipsoidal planet is profoundly different from motion on a spherical earth. Objects that are released from rest by an earthbound observer on a frictionless horizontal surface on our planet do not slide toward the equator, but instead remain at rest. Why? Because deforming a sphere into an ellipsoid effectively cancels the centrifugal force, which is absorbed into an "apparent" gravitational force, which is perpendicular to the ellipsoidal surface. So an object that is released from rest by an earthbound observer on a frictionless horizontal surface (defined as the local tangent to the ellipsoidal surface) experiences just two forces, the normal force and the apparent gravita-

tional force, and both of these forces are perpendicular to the surface. Hence the object remains at rest. Objects that move relative to the earthbound observer experience the Coriolis force, and execute small-amplitude "inertia oscillations" that keep them close to their initial latitudes [13, 30–32]. Observations of inertia oscillations in the oceans provide evidence of the Coriolis force [1].

In this paper, we present simple derivations of conservation principles that are key to the understanding of inertial forces for motion on the surface of the earth, for both spherical and ellipsoidal earths. The spherical earth is simpler, while the ellipsoidal earth better represents motion on our earth's surface. Given the 0.3% difference between the earth's equatorial and polar radii [33, p. 48], meteorologists sometimes argue that a spherical earth gives a good approximation for atmospheric models, forgetting that the spherical earth requires the centrifugal force, which is ignored in these models [34]. We study both earth shapes in order to dispel this misconception, and to emphasize the profound differences between motions on spherical and ellipsoidal earths.

*** John: The following information on visualizations has been copied from the NSF proposal, and needs to be trimmed for the paper, methinks. It's in no particular order. We need to find a balance between what we do in the paper and what we propose in the proposal. Would you like to have a go at trimming this section down to a paragraph or two?

Despite evidence that using multiple representations (verbal, mathematical, graphical, pictorial, and analogical) in instruction can increase student performance [35–38], and despite evidence that attending to student interpretations can increase student interest [39], at least one popular intermediate classical mechanics treatment of the Coriolis force presents the mathematics and little else [14].

Given the 0.3% difference between the earth's equatorial and polar radii [33, p. 48], meteorologists sometimes argue that a spherical earth gives a good approximation for atmospheric models, forgetting that the spherical earth requires the centrifugal force, which is ignored in these models [34].

Many simulations and visualizations specific to the Coriolis force can be found on the internet. Under NSF support, a set of animations were developed for a hockey puck "sliding without friction on a rotating spherical earth" [40]. These animations illustrate both the Coriolis and centrifugal forces and they show the inertial great circle, the path on the rotating earth, and the path on a stationary earth from the point of view of an inertial observer. The Exploring Earth visualization [41] by textbook publisher Houghton Mifflin shows a plane flying toward an intended target, but explains the effect using the Hadley principle, saying that "the target location where the plane was headed when it took off has moved with Earth's rotation, so the plane would end up to the right of its original target". The National Oceanic and Atmospheric Administration published a mini-lesson on the Coriolis effect showing an airplane simulation but they give no explanation beyond "because the earth is rotating" [42]. They do, however, include an interactive game, asking the student to predict where the airplane will land which can be used to confound misconceptions and assess student understanding. The [43] visualization demonstrates motion on a parabolic dish, with centripetal, centrifugal, and Coriolis force vectors. Replacing a flat rotating disk with a parabolic dish eliminates the centrifugal force for objects that are stationary as seen by an observer in the rotating frame, in the same way that replacing a spherical earth with an ellipsoidal earth eliminates the centrifugal force for objects that are stationary in the rotating frame. A large number of visualizations and demonstrations can be found on the web, e.g. [44], that demonstrate motion on a flat disc. Most of these demonstrations are not interactive, so the student cannot explore, ask questions, or self-assess understanding.

Despite evidence that physics students using simulated equipment can outperform their counterparts who use real equipment [45], and despite evidence that interactive simulations can be as productive as physical equipment or textbooks [46–48], currently available simulations and visualizations of Coriolis phenomena on the rotating earth are non-interactive, show no force vectors, and are restricted to the spherical earth and to one frame of reference [40]. Under NSF support, [40] developed a set of animations for motion on the spherical earth that serve as a useful starting point for our visualizations (Sec. **??**).

There is a critical need for instructional materials that clearly, simply, and correctly help students learn the physical origins of the Coriolis force, that present these explanations in a way that soundly dispels popular misconceptions, that correctly apply applicable conservation laws, that engage multiple representations and points of view, that include interactive feature-rich simulations and visualizations, that include physical in-class demonstrations, and that are widely available to the physics and earth science communities.

Interactive computer simulation to aid understanding of physics concepts is not a new idea. Prominent among these is the Physics Education Technology project, or PhET [49]. PhET began as a project to bring internet-based simulation to the Freshman Physics classroom with a structured development methodology based on careful design, strict coding standards, robust assessments, and broad accessibility. The usability design principles are open-play without requiring the student to read any instructions [50, 51]. While PhET has developed some simulations for more advanced courses [52], in recent years PhET has been moving more into the early intervention space, focusing on simulations for middle school and high school mathematics, physics and chemistry. The simulations are designed for high impact, to stimulate increased enrollments in collegiate STEM disciplines.

PhET was preceded by other interactive computer aids

to physics understanding. [53] developed a video analysis technique to assist in understanding kinematics. He confirmed the importance of interaction, saying, "hands-on involvement appeared to play a critical role.... Teacher-led demonstration resulted in no improvement in performance relative to traditional instruction." Another important set of simulations is Physlets, with simulations ranging from basic mechanics to thermodynamics to optics [54]. Each physlet is accompanied by a problem set to guide the student through interaction and generalization of the concept.

1. The McIntyre visualizations are animated but have no user interaction. This is partly due to technological constraints. We will be using HTML5 and WebGL and will design and build interactivity into the simulations from the very beginning. Learners will be able to speed up/slow down, pause, and reverse animations. We will provide simple controls to switch between preset frames of reference (e.g. inertial frame, rotating frame, object frame) and even allow the user to navigate to custom reference frames. The user will be able to run the simulation through time for as long as they wish, so in a simulation involving a great circle the great circle may be traced out multiple times, or in a simulation with no periodicity the path will continue to be traced as long as the user wishes.
2. Our visualizations will be rich with data, allowing the user to turn on/off momentum and force arrow overlays, tool-tips, and path tracings.
3. The design of our visualizations will be motivated by and grounded in actual Coriolis misconceptions. That is, our visualization design will be able to be traced directly back to specific Coriolis misconceptions that are identified and described in our misconception survey paper (see Section **??**).

Our physics simulations will be developed with the following guiding principles: ease-of-use, interaction, and understanding. The simulations must be easy to use in the sense that not only must the user interface be clear with little-to-no instruction, but they must be easy to access as well. Our simulations will be developed using Javascript and WebGL and will be entirely web-based. Users will not need to download or install additional software, but will be able to run the simulations inside a web browser. The user interface will be simple and entirely self-documenting, without the need for users to go through tutorials or read extra documentation. It will be an "open-play" environment where users can immediately engage in exploration.

The second guiding principle is interaction. Interaction engages students and, importantly, is highly effective if the interaction is driven by the student's own questioning [50, 51]. Demonstrative simulations have been used for many years, but only in recent years have interactive simulations been available, which allows the student to explore concepts rather than abstract only through thought experiments.

The third guiding principle is understanding, in that simulations are of little use if they are only entertaining. An approach to developing simulations that teach understanding is to design such that the simulation helps the student generalize the concept, or apply it in a different setting [55]. In order to enforce this in our simulations we will build in "formative assessments" [55], which assess understanding during the simulation rather than a posteriori, such as at the final exam. These assessments will take the form of instrumenting the student's interaction with the simulation. For example, how many times does the student repeat an action? How long is the student engaged with the simulation? How many features does the student explore? These assessments will be used during beta testing and deployed use for simulation refinement.

In contrast to the PhET simulations, our simulations will be customized to an upper-division undergraduate audience, with potential for more sophisticated visualizations. An example is our MagPhyx simulation, which renders velocity arrows, force arrows, moment, the underlying magnetic field and positional trace. While the interface is information-rich, care is taken not to distract the user from the most important features. However, the user is free to explore and modify a reasonably large set of parameters. At the same time, stock parameter sets are provided to acquaint the user with both the phenomena and the simulation. In MagPhyx, we provide 20+ stock simulations, each highlighting different phenomena. Included in the MagPhyx simulation parameters are toggles for different visualization features, so a stock simulation can not only run in a manner to highlight a phenomenon such as the unbounded spatial domain of the free magnet given the right set of initial conditions, but it can highlight the phenomenon further by turning on or off certain visualizations, such as a trace line of the free magnets position.

While care must be taken not to complicate the simulations, a feature-rich visualization enables users to explore complex mechanics phenomena, which necessarily take longer and more thought than simpler concepts at the introductory level. Further, simulation exploration by the student can also be thought of to do more than just communicate a concept, but it can be taken to the level of allowing the student to explore and even synthesize ideas. Our experience with MagPhyx, which was originally intended to be pedagogical but which led to core research in magnet dynamics [56], has shown that simulations can spur students to independent thinking and research. While allowing independent thought and exploration, controls and limitations will necessarily be built in so as to keep the simulation simple enough to ensure that less advanced students still have a pleasing educational experience. For example, numerical parameters will have bounds on them to disallow non-physical behavior that can distract students.

Simulation design will be done in collaboration be-

tween the PIs on this grant and software developers, taking into consideration data from instrumentation of simulations in beta test and possible user interviews. In this context, we use instrumentation to refer to computer code embedded into the software that measures usage statistics.

We will use a 3D vector graphics plotting library included with the three.js rendering library [57]... Other packages that are similar but generally offer only 2D plotting are [58] and [59]. Most web-based 3D visualization packages such as [60], [61], and [62] render using WebGL or directly using the HTML5 canvas element, so they don't have vector graphics resolution-independent rendering, an important components of our visualizations.

Simulation design and development will take place using an agile software development approach [63]. We will use iteration cycles of length 1-2 weeks, enabling us to keep the development progress visible to stakeholders as well as being able to catch issues early and often and adjust as needed. With the short iteration time, beta testers will get a new version of simulations frequently.

*** John: this is the end of the cutting and pasting from the proposal. The following paragraph, I think, will finish off the introduction:

Early [64] takes a Lagrangian approach to motion on the spherical and ellipsoidal earths, using constraint forces to confine the object to the surface. Our simpler force analysis, which is accessible to students of introductory physics and intermediate classical mechanics, allows us to easily identify the pertinent conservation principles and the frame (rotating or fixed) in which they apply. We use these principles to show that an object executes uniform circular motion on a frictionless spherical earth and inertia oscillations on a frictionless ellipsoidal earth, and obtain the frequency for small-amplitude inertia oscillations. We also present five fundamental concepts needed to understand inertial forces and to explain Coriolis deflections in a straightforward way, for both spherical and ellipsoidal earths. We also introduce new high-quality, feature-rich visualizations intended to assist students and teachers of physics and earth science to understand these deflections, and make these visualizations freely available online.

II. DYNAMICS

As seen by an observer in a "fixed" inertial frame S_0, looking down from space upon the rotating earth, an object of mass m that slides without friction along the surface of the earth satisfies Newton's second law,

$$m\left(\frac{d^2\mathbf{r}}{dt^2}\right)_{S_0} = \mathbf{F}_\mathrm{g} + \mathbf{F}_\mathrm{n}, \tag{1}$$

where $\mathbf{F}_\mathrm{g}$ and $\mathbf{F}_\mathrm{n}$ are the gravitational and normal forces on the object, $\mathbf{r}$ is its position, and

$$\left(\frac{d^2\mathbf{r}}{dt^2}\right)_{S_0} \tag{2}$$

is its acceleration as seen by an observer in this frame.

We also consider a "rotating" non-inertial frame S that rotates with the earth's angular velocity $\mathbf{\Omega}$ relative to the fixed frame. To transform Eq. (1) into this frame, we need [14, Ch. 9]

$$\left(\frac{d\mathbf{Q}}{dt}\right)_{S_0} = \left(\frac{d\mathbf{Q}}{dt}\right)_{S} + \mathbf{\Omega}\times\mathbf{Q}, \tag{3}$$

where

$$\left(\frac{d\mathbf{Q}}{dt}\right)_{S_0} \tag{4}$$

is the rate of change of a vector $\mathbf{Q}$ as observed in the fixed frame and

$$\left(\frac{d\mathbf{Q}}{dt}\right)_{S} \tag{5}$$

is the rate of change of the same vector $\mathbf{Q}$ as observed in the rotating frame. Setting $\mathbf{Q} = \mathbf{r}$ in Eq. (3) gives a relationship between the velocities measured by observers in the two frames,

$$\left(\frac{d\mathbf{r}}{dt}\right)_{S_0} = \left(\frac{d\mathbf{r}}{dt}\right)_{S} + \mathbf{\Omega}\times\mathbf{r}. \tag{6}$$

Differentiating Eq. (6) and applying Eq. (3) gives a relationship between the accelerations measured by observers in the two frames,

$$\left(\frac{d^2\mathbf{r}}{dt^2}\right)_{S_0} = \left(\frac{d}{dt}\right)_{S_0}\left[\left(\frac{d\mathbf{r}}{dt}\right)_{S} + \mathbf{\Omega}\times\mathbf{r}\right] \tag{7}$$

$$= \left[\left(\frac{d}{dt}\right)_{S} + \mathbf{\Omega}\times\right]\left[\left(\frac{d\mathbf{r}}{dt}\right)_{S} + \mathbf{\Omega}\times\mathbf{r}\right] \tag{8}$$

$$= \left(\frac{d^2\mathbf{r}}{dt^2}\right)_{S} + 2\mathbf{\Omega}\times\left(\frac{d\mathbf{r}}{dt}\right)_{S} + \mathbf{\Omega}\times(\mathbf{\Omega}\times\mathbf{r}) \tag{9}$$

Inserting Eq. (9) into Eq. (1) gives a modified form of Newton's second law that applies in the rotating frame,

$$m\left(\frac{d^2\mathbf{r}}{dt^2}\right)_{S} = \mathbf{F}_\mathrm{g} + \mathbf{F}_\mathrm{n} + \mathbf{F}_\mathrm{cor} + \mathbf{F}_\mathrm{cen}, \tag{10}$$

where the Coriolis force

$$\mathbf{F}_\mathrm{cor} = -2m\mathbf{\Omega}\times\left(\frac{d\mathbf{r}}{dt}\right)_{S} \tag{11}$$

and the centrifugal force

$$\mathbf{F}_\mathrm{cen} = -m\mathbf{\Omega}\times(\mathbf{\Omega}\times\mathbf{r}) \tag{12}$$

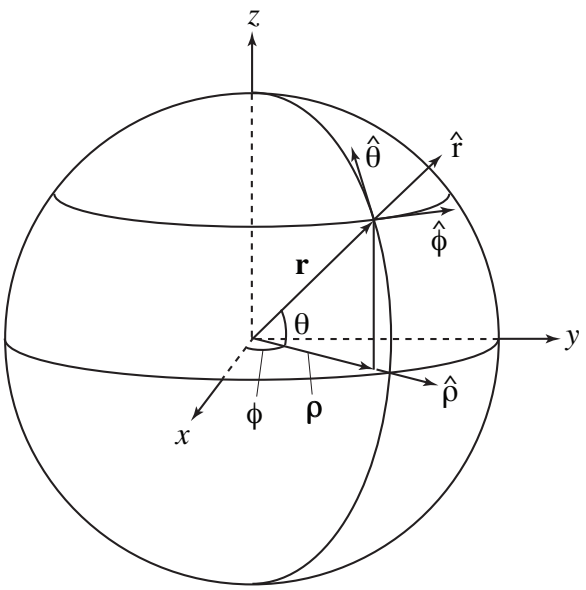

FIG. 1. Spherical coordinates in the rotating (non-inertial) reference frame that rotates with the earth's angular velocity $\mathbf{\Omega} = \Omega\hat{\mathrm{z}}$ about the fixed frame. In the rotating frame, the coordinate unit vectors $\hat{\mathrm{x}}$, $\hat{\mathrm{y}}$, and $\hat{\mathrm{z}}$ are stationary with respect to an earthbound observer, and point to specific, unchanging geographical locations on the earth's surface. Positions $\mathbf{r}$ are specified by a longitude ϕ, latitude θ, and distance r from the earth's center, with corresponding unit vectors $\hat{\phi}$, $\hat{\theta}$, and $\hat{\mathrm{r}}$ pointing east, north, and up for a spherical earth.

are "inertial" forces on the object that apply only in the rotating frame. These inertial forces augment the normal and gravitational forces that also apply in the fixed frame. Intermediate (upper-division) classical mechanics students learn how to perform the coordinate transformation used above to obtain Eq. (10), and learn how to calculate deflections produced by the inertial forces for motions near the earth's surface [14, Ch. 9].

It is convenient to write the position vector

$$\mathbf{r} = x\hat{\mathrm{x}} + y\hat{\mathrm{y}} + z\hat{\mathrm{z}} = r\hat{\mathrm{r}} \tag{13}$$

in spherical coordinates in the rotating frame, with $\hat{\mathrm{x}}$, $\hat{\mathrm{y}}$, and $\hat{\mathrm{z}}$ rotating with the earth, as seen by an observer in the fixed frame. As seen by an observer in the rotating frame, these vectors are stationary, and point toward specific, unchanging geographical locations on the earth's surface, with $\hat{\mathrm{x}}$ and $\hat{\mathrm{y}}$ pointing toward fixed locations at the equator and with $\hat{\mathrm{z}}$ pointing toward the north pole and giving the direction of the earth's angular velocity (Fig. 1):

$$\mathbf{\Omega} = \Omega\hat{\mathrm{z}}. \tag{14}$$

We measure the latitude θ northward from the equator and the longitude ϕ eastward from the prime meridian, giving coordinates

$$x = r\cos\phi\cos\theta \tag{15}$$
$$y = r\sin\phi\cos\theta \tag{16}$$
$$z = r\sin\theta. \tag{17}$$

The unit vectors

$$\hat{\phi} = -\sin\phi\hat{\mathrm{x}} + \cos\phi\hat{\mathrm{y}} \tag{18}$$
$$\hat{\theta} = -\sin\theta\cos\phi\hat{\mathrm{x}} - \sin\theta\sin\phi\hat{\mathrm{y}} + \cos\theta\hat{\mathrm{z}} \tag{19}$$
$$\hat{\mathrm{r}} = \cos\theta\cos\phi\hat{\mathrm{x}} + \cos\theta\sin\phi\hat{\mathrm{y}} + \sin\theta\hat{\mathrm{z}} \tag{20}$$

form a right-handed coordinate system, and respectively point east, north, and up for a spherical earth. The projection of $\mathbf{r}$ onto the x-y plane gives $\boldsymbol{\rho} = \rho\hat{\rho}$, where

$$\rho = r\cos\theta \tag{21}$$

gives the distance to the z axis, and

$$\hat{\rho} = \cos\phi\hat{\mathrm{x}} + \sin\phi\hat{\mathrm{y}} \tag{22}$$

points away from the z axis.

Because $\hat{\mathrm{x}}$, $\hat{\mathrm{y}}$, and $\hat{\mathrm{z}}$ are stationary in the rotating frame, the velocity measured in this frame is [Eq. 13]

$$\left(\frac{d\mathbf{r}}{dt}\right)_S = \left(\frac{dx}{dt}\right)_S\hat{\mathrm{x}} + \left(\frac{dy}{dt}\right)_S\hat{\mathrm{y}} + \left(\frac{dz}{dt}\right)_S\hat{\mathrm{z}} \tag{23}$$
$$= \rho\left(\frac{d\phi}{dt}\right)_S\hat{\phi} + r\left(\frac{d\theta}{dt}\right)_S\hat{\theta} + \left(\frac{dr}{dt}\right)_S\hat{\mathrm{r}} \tag{24}$$
$$= v_\phi\hat{\phi} + v_\theta\hat{\theta} + v_r\hat{\mathrm{r}}. \tag{25}$$

Equation (24) can be readily verified using Eqs. (15)-(20).

The Coriolis force, given by Eq. (11), is perpendicular to the plane formed by $\mathbf{\Omega}$ and $(d\mathbf{r}/dt)_S$, and applies only for objects that are moving relative to the rotating frame. In contrast, the centrifugal force applies in the rotating frame for both stationary and moving objects. Rewriting Eq. (12) demonstrates that this force is directed away from the earth's axis, according to

$$\mathbf{F}_{\mathrm{cen}} = m\Omega^2\boldsymbol{\rho} \tag{26}$$

For a uniform spherical earth, the force of gravity on a mass m at a distance r from the earth's center is given by

$$\mathbf{F}_{\mathrm{g}} = -\boldsymbol{\nabla}U_{\mathrm{g}}, \tag{27}$$

with the gravitational potential energy given by

$$U_{\mathrm{g}} = -\frac{mMG}{r}, \tag{28}$$

where M is the earth mass and G is Newton's gravitational constant. Consequently, the gravitational force

$$\mathbf{F}_{\mathrm{g}} = -\frac{dU_{\mathrm{g}}}{dr}\hat{\mathrm{r}} \tag{29}$$
$$= -\frac{mMG}{r^2}\hat{\mathrm{r}} \tag{30}$$

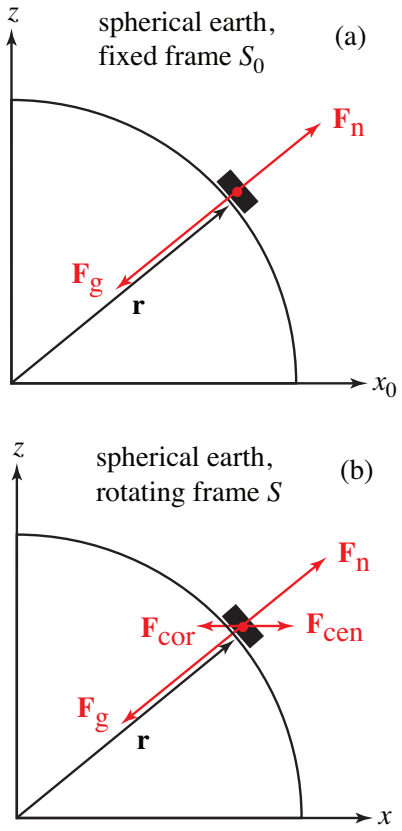

FIG. 2. Diagram showing the forces acting on a puck sliding on a frictionless spherical earth as seen by observers in the fixed frame (a) and the rotating frame (b), with the Coriolis force shown for westward motion (out of the plane of the figure).

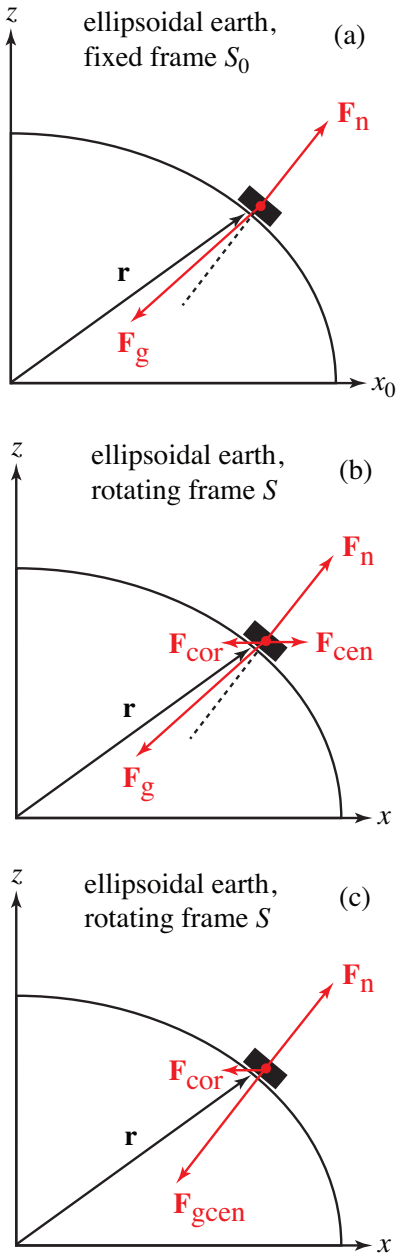

FIG. 3. Diagram showing the forces acting on a puck sliding on a frictionless ellipsoidal earth as seen by observers in the fixed frame (a) and the rotating frame (b,c), with the Coriolis force shown for westward motion. The non-sphericity of the earth is exaggerated in the figure.

is radially inward, or "central," and is perpendicular to the earth's surface. The normal force $\mathbf{F}_n = F_n\hat{\mathbf{r}}$ is also perpendicular to this surface (Fig. 2). A hockey puck that is released from rest in the rotating frame on the surface of a frictionless spherical earth will experience a centrifugal force that drives it toward the equator (Fig. 3b).

On our ellipsoidal earth, pucks that are released from rest on horizontal frictionless surfaces do not slide toward the equator. They remain at rest. This is because the sum of the gravitational and centrifugal forces,

$$\mathbf{F}_{gcen} = \mathbf{F}_g + \mathbf{F}_{cen}, \tag{31}$$

is perpendicular to the earth's ellipsoidal surface (Fig. 3). Historically, the earth acquired its ellipsoidal shape as a result of the centrifugal force, which deformed the surface until it was everywhere perpendicular to $\mathbf{F}_{gcen}$. Consequently, a hockey puck that is released from rest in the rotating frame on the surface of a frictionless ellipsoidal earth will remain at rest (Fig. 3c), and objects released from rest above the earth's surface experience an initial acceleration that is parallel to $\mathbf{F}_{gcen}$ and perpendicular to the earth's surface [14, 30]. The horizontal plane is defined as the plane that is locally tangent to this surface.

For an ellipsoidal earth of mass M and a point mass m, the approximate gravitational potential energy is [33, p. 48][65, Ch. 6]

$$U_g = -\frac{mMG}{r}\left[1 - J_2\frac{R_e^2}{r^2}P_2(\sin\theta)\right], \tag{32}$$

where R_e is the equatorial radius,

$$P_2(\sin\theta) = \frac{1}{2}\left(3\sin^2\theta - 1\right) \tag{33}$$

is the second Legendre function, $J_2 = 1.083 \times 10^{-3}$ characterizes the earth's deviation from sphericity, and the equatorial and polar radii satisfy $(R_\mathrm{e} - R_\mathrm{p})/R_\mathrm{e} = 3.35 \times 10^{-3}$. Inserting Eq. (32) into Eq. (27) yields the corresponding gravitational force

$$\mathbf{F}_\mathrm{g} = -\frac{\partial U_\mathrm{g}}{\partial r}\hat{\mathrm{r}} - \frac{1}{r}\frac{\partial U_\mathrm{g}}{\partial \theta}\hat{\theta} \tag{34}$$

$$= -\frac{mMG}{r^2}\left[1 - 3J_2\frac{R_\mathrm{e}^2}{r^2}P_2(\sin\theta)\right]\hat{\mathrm{r}} \tag{35}$$

$$-\frac{3mMGJ_2R_\mathrm{e}^2}{2r^4}\sin(2\theta)\hat{\theta} \tag{36}$$

The gravitational force $\mathbf{F}_\mathrm{g}$ of the ellipsoidal earth is not directed radially inward toward the earth's center (because of the $\hat{\theta}$ component), nor is it normal to the ellipsoidal surface (because $\mathbf{F}_\mathrm{gcen}$ is normal to this surface and $\mathbf{F}_\mathrm{g} = \mathbf{F}_\mathrm{gcen} - \mathbf{F}_\mathrm{cen}$). Consequently, the direction of $\mathbf{F}_\mathrm{g}$ is intermediate between the radially inward and normal directions (Fig. 3b).

III. ANGULAR MOMENTUM CONSERVATION

In this section, we show that the axial component of angular momentum of a hockey puck sliding along the frictionless surface of the earth is conserved in the fixed frame of reference, for both spherical and ellipsoidal earths.

The angular momentum of a particle of mass m is defined as

$$\mathbf{L} = \mathbf{r} \times \mathbf{p}, \tag{37}$$

where

$$\mathbf{p} = m\frac{d\mathbf{r}}{dt} \tag{38}$$

is its linear momentum. The time derivative of this angular momentum is given by

$$\frac{d\mathbf{L}}{dt} = \frac{d\mathbf{r}}{dt} \times \mathbf{p} + \mathbf{r} \times \frac{d\mathbf{p}}{dt}. \tag{39}$$

The first term on the right side vanishes because $\mathbf{p}$ is parallel to $d\mathbf{r}/dt$, leaving

$$\frac{d\mathbf{L}}{dt} = \mathbf{r} \times \frac{d\mathbf{p}}{dt}. \tag{40}$$

The axial component of the angular momentum

$$L_z = \hat{\mathrm{z}} \cdot \mathbf{L} \tag{41}$$

therefore satisfies

$$\frac{dL_z}{dt} = \hat{\mathrm{z}} \cdot \left(\mathbf{r} \times \frac{d\mathbf{p}}{dt}\right) \tag{42}$$

$$= \frac{d\mathbf{p}}{dt} \cdot (\hat{\mathrm{z}} \times \mathbf{r}) \tag{43}$$

$$= \left(m\frac{d^2\mathbf{r}}{dt^2}\right) \cdot \rho\hat{\phi} \tag{44}$$

where we have permuted the triple product in the second step, and we have used Eq. (38) and

$$\hat{\mathrm{z}} \times \mathbf{r} = \rho\hat{\phi} \tag{45}$$

in the third step (Fig. 1). The term in parentheses in the last step is the net force on the puck.

We can evaluate Eq. (44) in the rotating frame by inserting the net force given by Eq. (10), yielding

$$\left(\frac{dL_z}{dt}\right)_S = \rho\hat{\phi} \cdot (\mathbf{F}_\mathrm{g} + \mathbf{F}_\mathrm{n} + \mathbf{F}_\mathrm{cor} + \mathbf{F}_\mathrm{cen}). \tag{46}$$

Because $\mathbf{F}_\mathrm{g}$, $\mathbf{F}_\mathrm{n}$, and $\mathbf{F}_\mathrm{cen}$ are in the plane formed by the position of the puck and the z axis, and because $\hat{\phi}$ is perpendicular to this plane, the scalar products with these forces vanish on the right side of Eq. (46) (see Figs. 2b, 3b). But if $(d\mathbf{r}/dt)_S$ has a $\hat{\theta}$ component, then $\mathbf{F}_\mathrm{cor}$ will be out of this plane, and the scalar product $\hat{\phi} \cdot \mathbf{F}_\mathrm{cor}$ will not be zero. Therefore, the axial angular momentum is not conserved in the rotating frame.

We can evaluate Eq. (44) in the fixed frame by inserting the net force given by Eq. (1), yielding

$$\left(\frac{dL_z}{dt}\right)_{S_0} = \rho\hat{\phi} \cdot (\mathbf{F}_\mathrm{g} + \mathbf{F}_\mathrm{n}). \tag{47}$$

Both forces in the fixed frame are in the plane formed by the position of the puck and the z axis (see Figs. 2a, 3a), so both scalar products vanish and axial angular momentum is conserved:

$$\left(\frac{dL_z}{dt}\right)_{S_0} = 0. \tag{48}$$

Thus, the axial angular momentum of the puck is conserved in the fixed frame for motion on both the spherical and ellipsoidal earths.

Combining Eqs. (37), (38), and (41) allows us to

rewrite this angular momentum as

$$(L_z)_{S_0} = \hat{\mathrm{z}} \cdot \left[\mathbf{r} \times m \left(\frac{d\mathbf{r}}{dt} \right)_{S_0} \right] \tag{49}$$

$$= m \left(\frac{d\mathbf{r}}{dt} \right)_{S_0} \cdot (\hat{\mathrm{z}} \times \mathbf{r}) \tag{50}$$

$$= m\rho \left(\frac{d\mathbf{r}}{dt} \right)_{S_0} \cdot \hat{\phi} \tag{51}$$

$$= m\rho \left[\left(\frac{d\mathbf{r}}{dt} \right)_{S} + (\boldsymbol{\Omega} \times \mathbf{r}) \right] \cdot \hat{\phi} \tag{52}$$

$$= m\rho \left(\frac{d\mathbf{r}}{dt} \right)_{S} \cdot \hat{\phi} + m\rho^2 \Omega \tag{53}$$

$$= m\rho^2 \left[\Omega + \left(\frac{d\phi}{dt} \right)_{S} \right], \tag{54}$$

where we have used Eqs. (6), (14), (24), and (45) to write this angular momentum using convenient time derivatives in the rotating frame.

For the elliptical earth, only the axial component of the angular momentum is conserved in the fixed frame, but for the spherical earth, all components of the angular momentum are conserved in the fixed frame. This is easily seen by evaluating Eq. (40) in the fixed frame,

$$\left(\frac{d\mathbf{L}}{dt} \right)_{S_0} = \mathbf{r} \times (\mathbf{F}_{\mathrm{g}} + \mathbf{F}_{\mathrm{n}}) \,. \tag{55}$$

Both vector products on the right side are in the $\hat{\phi}$ direction for the ellipsoidal earth (Fig. 3a), meaning that the $\hat{\mathrm{x}}$ and $\hat{\mathrm{y}}$ components of the angular momentum are not conserved (though the $\hat{\mathrm{z}}$ component is conserved because it is perpendicular to $\hat{\phi}$. For the spherical earth, both cross products on the right side vanishe because $\mathbf{F}_{\mathrm{g}}$ and $\mathbf{F}_{\mathrm{n}}$ are parallel to $\mathbf{r}$ for the spherical earth (Fig. 2a).

IV. CONSERVATION OF KINETIC ENERGY

In this section, we show that the kinetic energy of a hockey puck sliding along the frictionless surface of the earth is conserved in the fixed frame for a spherical earth, and is conserved in the rotating frame for an ellipsoidal earth.

In the **fixed frame**, the kinetic energy is given by

$$(T)_{S_0} = \frac{1}{2} m \left(\frac{d\mathbf{r}}{dt} \right)_{S_0}^2 , \tag{56}$$

and its time rate of change is given by

$$\left(\frac{dT}{dt} \right)_{S_0} = m \left(\frac{d\mathbf{r}}{dt} \right)_{S_0} \cdot \left(\frac{d^2\mathbf{r}}{dt^2} \right)_{S_0} \tag{57}$$

$$= (\mathbf{F}_{\mathrm{g}} + \mathbf{F}_{\mathrm{n}}) \cdot \left(\frac{d\mathbf{r}}{dt} \right)_{S_0} , \tag{58}$$

where we have inserted the net force given by Eq. (1). The right side vanishes on the spherical earth because the puck velocity is tangent to the earth's surface and the two forces are perpendicular to the surface (Fig. 2a), leaving

$$\left(\frac{dT}{dt} \right)_{S_0} = 0 \tag{59}$$

for the spherical earth. Thus, the puck's kinetic energy is conserved in the fixed frame for motion on a frictionless spherical earth. Equations (6) and (24) allow us to write the conserved kinetic energy in the fixed frame for motion on a frictionless spherical earth [Eq. (56)] using time derivatives in the rotating frame,

$$(T)_{S_0} = \frac{1}{2} m \left\{ \rho^2 \left[\Omega + \left(\frac{d\phi}{dt} \right)_{S} \right]^2 + r^2 \left(\frac{d\theta}{dt} \right)_{S}^2 + \left(\frac{dr}{dt} \right)_{S}^2 \right\} \tag{60}$$

In the **rotating frame**, the kinetic energy is given by

$$(T)_{S} = \frac{1}{2} m \left(\frac{d\mathbf{r}}{dt} \right)_{S}^2 , \tag{61}$$

and its time rate of change is given by

$$\left(\frac{dT}{dt} \right)_{S} = m \left(\frac{d\mathbf{r}}{dt} \right)_{S} \cdot \left(\frac{d^2\mathbf{r}}{dt^2} \right)_{S} \tag{62}$$

$$= (\mathbf{F}_{\mathrm{gcen}} + \mathbf{F}_{\mathrm{n}} + \mathbf{F}_{\mathrm{cor}}) \cdot \left(\frac{d\mathbf{r}}{dt} \right)_{S} , \tag{63}$$

where we have used Eqs. (10) and (31) for the net force. The scalar products with $\mathbf{F}_{\mathrm{gcen}}$ and $\mathbf{F}_{\mathrm{n}}$ vanish on the ellipsoidal earth because the puck velocity is tangent to the surface and these two forces are perpendicular to the surface (Fig. 3c). The scalar product with $\mathbf{F}_{\mathrm{cor}}$ satisfies

$$\mathbf{F}_{\mathrm{cor}} \cdot \left(\frac{d\mathbf{r}}{dt} \right)_{S} = -2m \left[\boldsymbol{\Omega} \times \left(\frac{d\mathbf{r}}{dt} \right)_{S} \right] \cdot \left(\frac{d\mathbf{r}}{dt} \right)_{S} \tag{64}$$

$$= -2m \left[\left(\frac{d\mathbf{r}}{dt} \right)_{S} \times \left(\frac{d\mathbf{r}}{dt} \right)_{S} \right] \cdot \boldsymbol{\Omega} \tag{65}$$

$$= 0 \tag{66}$$

where we have inserted Eq. (11) and we have permuted the triple product. Thus,

$$\left(\frac{dT}{dt} \right)_{S} = 0, \tag{67}$$

implying that the puck's kinetic energy is conserved in the rotating frame for motion on a frictionless ellipsoidal earth. Equation (24) allows us to write the conserved kinetic energy in the rotating frame of a frictionless ellipsoidal earth [Eq. (61)] as

$$(T)_{S} = \frac{1}{2} m \left[\rho^2 \left(\frac{d\phi}{dt} \right)_{S}^2 + r^2 \left(\frac{d\theta}{dt} \right)_{S}^2 + \left(\frac{dr}{dt} \right)_{S}^2 \right] \tag{68}$$

V. SPHERICAL EARTH

On the frictionless spherical earth, the total angular momentum and the kinetic energy of a puck are conserved in the fixed frame. Consequently, the puck executes uniform circular motion in a great circle around the earth, as viewed in the fixed frame.

To enable us to track the position of the puck on the surface of the rotating earth, we replace time derivatives $(d/dt)_S$ by an overdot and set $r = R$ in Eqs. (54) and (60), yielding

$$L_0 = \left(\Omega + \dot{\phi}\right) \cos^2\theta \tag{69}$$

$$T_0 = \left(\Omega + \dot{\phi}\right)^2 \cos^2\theta + \dot{\theta}^2, \tag{70}$$

where

$$L_0 \equiv \frac{1}{mR^2} \left(L_z\right)_{S_0} \tag{71}$$

$$T_0 \equiv \frac{2}{mR^2} \left(T\right)_{S_0} \tag{72}$$

are constants of the motion. Equations (69) and (70) respectively express conservation of axial angular momentum and conservation of kinetic energy in the fixed frame.

Since the motion on the spherical earth is simple in the fixed frame and since both of its conservation laws apply in this frame, it is convenient to study motion on the sphere using

$$\Phi = \phi + \Omega t \tag{73}$$

to measure the azimuthal angle as seen by an observer in this frame. Consequently, Eqs. (69) and (70) take the simpler forms

$$L_0 = \dot{\Phi} \cos^2\theta \tag{74}$$

$$T_0 = \dot{\Phi}^2 \cos^2\theta + \dot{\theta}^2. \tag{75}$$

Equations (69) and (70) are nonlinear, coupled, first-order equations describing motion of a puck on the surface of a frictionless spherical earth in the fixed frame, with the positions of the puck specified in this frame by the azimuthal angle $\Phi(t)$ and the latitude $\theta(t)$. We solve these equations in two special cases.

Case 1 is to release the puck from rest ($\dot{\theta} = \dot{\phi} = 0$) from latitude $\theta = \theta_0$ and longitude $\phi = 0$ in the rotating frame. As seen by an observer in the fixed frame, the puck has an initial eastward velocity of magnitude $v = \Omega R \cos\theta_0$ because it rotates with the earth. After the puck is released, it executes uniform circular motion around the center of the earth, as seen by an observer in this frame, with period $\tau = 2\pi R/v = \tau_e/\cos\theta_0$, where $\tau_e = 2\pi/\Omega$ is the rotation period of the earth (24 h). As the puck moves along a great circle, it passes point C at $t = 0$ and point B at time t (Fig. 4). This great circle and the two longitude circles that pass through points C and B form a right spherical triangle ABC, with angle

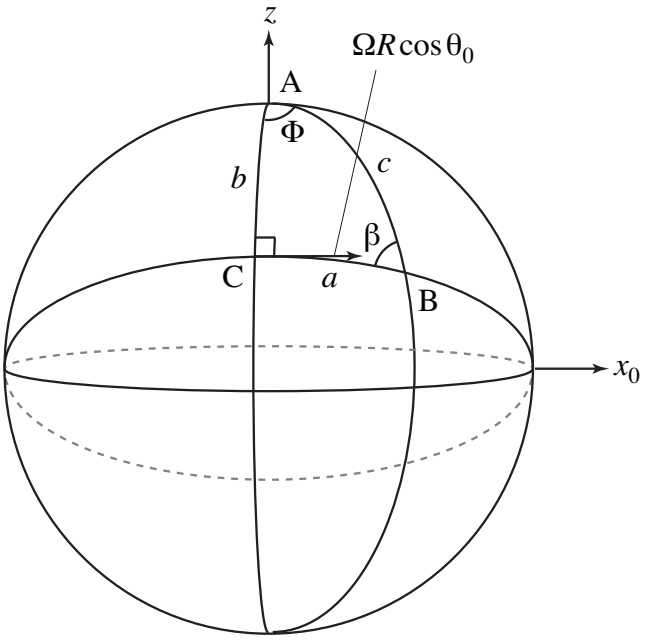

FIG. 4. Diagram showing the path of a puck that is released from rest as seen by an observer in the rotating frame, at point C at latitude θ_0 on a frictionless spherical earth. The figure is shown in the fixed frame, in which the puck has eastward velocity $v = \Omega R \cos\theta_0$ because it is moving with the rotating earth, of radius R and angular speed Ω. From point C, the puck slides to point B and continues around the great circle shown.

Φ at point A, the north pole, angle β at point B, and a right angle at point C. The arc length $a = R\delta$ subtends the angle δ through which the puck travels during time t, the arc length $b = R(\pi/2 - \theta_0)$ subtends the initial polar angle $\pi/2 - \theta_0$, and the arc length $c = R(\pi/2 - \theta)$ subtends the final polar angle $\pi/2 - \theta$. As seen by an observer in the fixed frame, a puck traveling with speed v from C to B travels a distance $a = vt$ during a time t. Napier Rules 1 and 4 immediately yield solutions for $\theta(t)$ and $\Phi(t)$ [66],

$$\sin\theta = \sin\theta_0 \cos\frac{vt}{R} \tag{76}$$

$$\tan\Phi = \frac{1}{\cos\theta_0} \tan\frac{vt}{R}. \tag{77}$$

These solutions satisfy Eqs. (74) and (75), with constants $L_0 = \Omega\cos^2\theta_0$ and $T_0 = \Omega^2\cos^2\theta_0$, and track the uniform circular motion of the puck around the earth's surface. The puck starts at north latitude $\theta = \theta_0$ at time $t = 0$, passes through the equator at time $t = \tau/4$, reaches south latitude $\theta = -\theta_0$ at time $t = \tau/2$, passes back through the equator at time $t = 3\tau/4$, and returns to its starting point (as seen by an observer in the fixed frame) at $t = \tau$. Because the earth rotates underneath the puck as it executes this great circle, the puck does not generally return to the same geographical location on the earth.

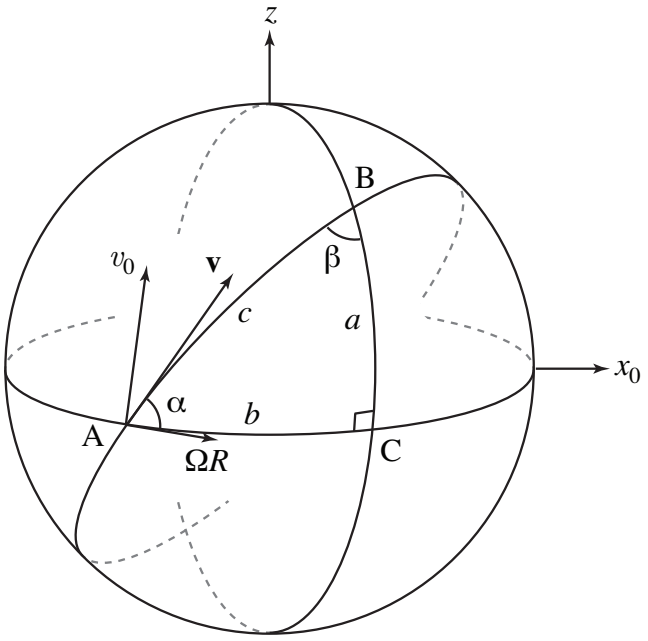

FIG. 5. Diagram showing the path of a puck that is launched from point A at the equator due north with speed v_0 as seen by an observer in the rotating frame, on a frictionless spherical earth. The figure is shown in the fixed frame, in which the puck also has an eastward component of velocity ΩR because it is moving with the rotating earth. From point A, the puck slides to point B, whose longitude circle makes a right angle with the equator at point C, and continues around the great circle shown.

Evidently, a puck that is released from rest in the rotating frame on the surface of a spherical frictionless earth does not remain at rest, and instead visits both hemispheres equally. In the rotating frame, the Coriolis and centrifugal forces are responsible for this motion, while in the fixed frame, the motion is eminently simple.

Case 2 is to launch the puck due north from at the equator with initial speed v_0, as seen by an observer in the rotating frame. As seen by an observer in the fixed frame, the puck has two components of velocity, a component ΩR toward the east because it is moving with the rotating earth, and its component v_0 toward the north (Fig. 5). As seen by this observer, the puck's speed

$$v = \sqrt{v_0^2 + \Omega^2 R^2} \tag{78}$$

is constant as it executes uniform circular motion in a great circle around the earth's center. Its launch angle is given by

$$\tan\alpha = \frac{v_0}{\Omega R}. \tag{79}$$

The puck departs from point A at time $t = 0$ and arrives at point B at time t, whose longitude circle makes a right angle with the equator at point C. Thus, triangle ABC is a spherical right triangle, forming angles α and β at points A and B. The arc length $a = R\theta$ subtends the latitude θ, the arc length $b = R\Phi$ subtends the azimuthal angle Φ, and the arc length $c = R\delta$ subtends an angle δ. As seen by an observer in the fixed frame, the puck travels a distance $c = vt$ from A to B during a time t, whence Napier Rules 2 and 6 give solutions for $\theta(t)$ and $\Phi(t)$ [66],

$$\sin\theta = \frac{v_0}{v}\sin\frac{vt}{R} \tag{80}$$

$$\tan\Phi = \frac{\Omega R}{v}\tan\frac{vt}{R}. \tag{81}$$

These solutions satisfy Eqs. (74) and (75), with constants $L_0 = \Omega$ and $T_0 = v^2/R^2$ that are consistent with the initial conditions $\theta = 0$, $\dot\theta = v_0/R$, $\Phi = 0$, and $\dot\Phi = \Omega$.

Shown in Fig. (6) are a sequence of snapshots from a visualization of Case 2 with $v_0 = \sqrt{5/4}\,\Omega R$, $v = (3/2)\Omega R$, and $\tau = 2\pi R/v = (2/3)\tau_e = 16$ h. The puck takes 4 h to travel from the equator to its maximum northern latitude $\theta_{\max} = \alpha = \tan^{-1}\sqrt{5/4} = 48°$, 4 h to travel back to the equator, 4 h to travel to its maximum southern latitude -48°, and 4 h to travel back to the equator. During this 16 h period, the earth completes only 2/3 of its daily 24 h rotation.

VI. ELLIPSOIDAL EARTH

On the frictionless ellipsoidal earth, the axial angular momentum of the puck is conserved in the fixed frame and the kinetic energy of the puck is conserved in the rotating frame. To study the motion of the puck, we again replace time derivatives $(d/dt)_S$ by an overdot and set $r = R$, whence Eqs. (54) and (68) give

$$L_0 = \left(\Omega + \dot\phi\right)\cos^2\theta \tag{82}$$

$$T = \dot\phi^2\cos^2\theta + \dot\theta^2, \tag{83}$$

where

$$L_0 = \frac{1}{mR^2}\,(L_z)_{S_0} \tag{84}$$

$$T = \frac{2}{mR^2}\,(T)_S \tag{85}$$

are constants of the motion. Equations (82) and (83) respectively express conservation of axial angular momentum in the fixed frame and conservation of kinetic energy in the rotating frame.

Equation (82) is identical to Eq. (69) for motion on the spherical earth. But the factor $\dot\phi^2$ in Eq. (83) is generally much smaller than the factor $(\Omega+\dot\phi)^2$ in Eq. (70) for the spherical earth. This is because the rate of change of longitude $\dot\phi$ for motion on the earth's surface is generally much smaller than the earth's angular velocity Ω. The marked difference between Eqs. (83) and (70) stems from the absorption of the centrifugal force into the apparent

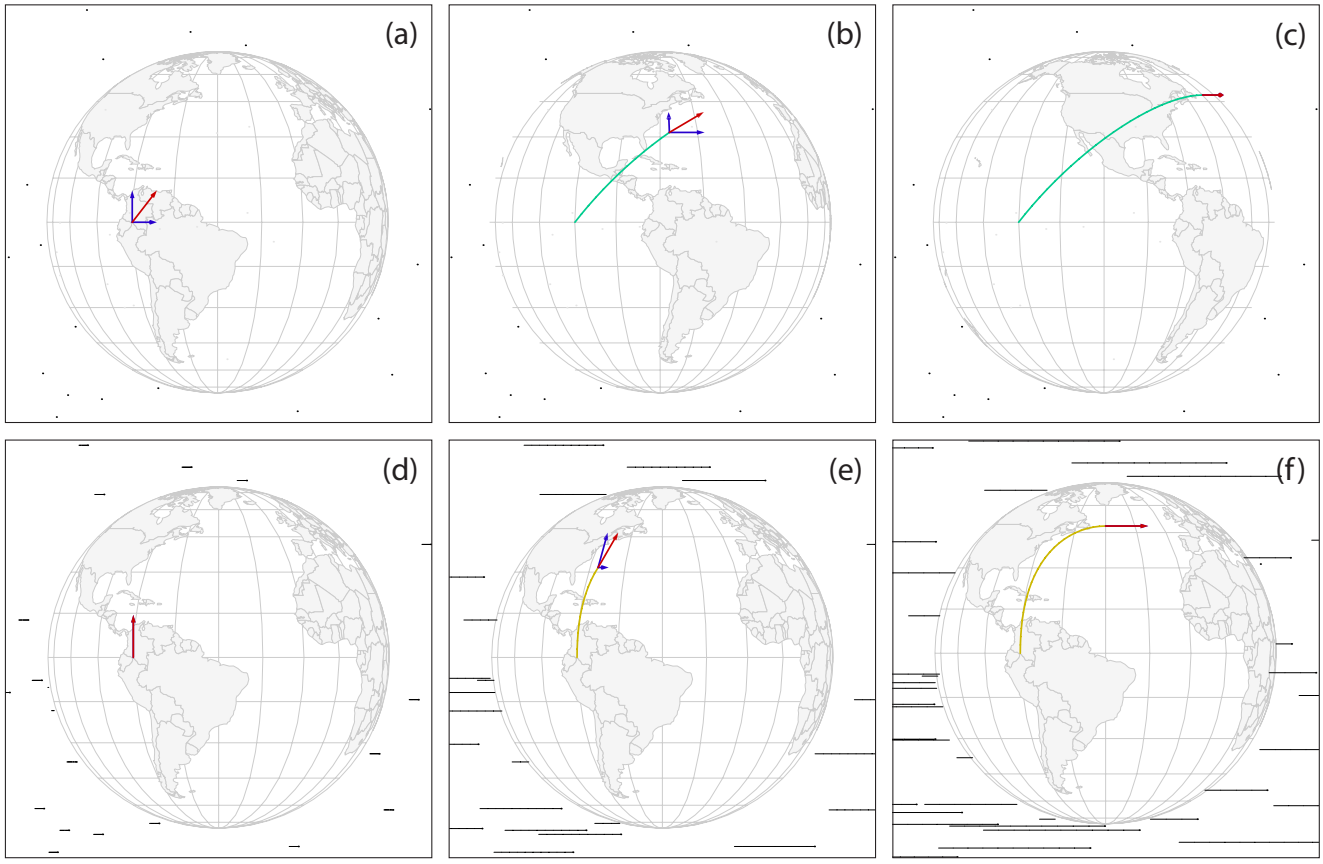

FIG. 6. Diagram showing the path of a puck that is launched from the equator due north with speed $v_0 = \sqrt{5/4}\,\Omega R$ as seen by an observer in the rotating frame, on a frictionless spherical earth of radius R and angular velocity Ω. As seen by an observer in the fixed frame, the puck has an initial eastward component of velocity ΩR because it is moving with the rotating earth. Panels (a), (b), and (c) show the puck positions and velocities at times $t = 0$, 2 h, and 4 h in the fixed frame, and panels (d), (e), and (f) show the puck positions and velocities at these times in the rotating frame. During these 4 hours, the earth rotates 60° toward the east, as can be seen in panels (a)-(c). (Longitude circles and latitude lines are drawn every 15°.)

gravitational force on the ellipsoidal earth. This difference has profound consequences for the motion, as will be seen below.

Equations (82) and (83) ignore the tiny latitude dependence of the earth's radius [33, p. 48], acknowledging that the difference between Eq. (83) and (70) provides the crucial difference between the ellipsoidal and spherical earths.

We now consider the motion of the puck on the ellipsoidal earth for the initial conditions $\phi = \phi_0$, $\theta = \theta_0$, $v_\phi = 0$, and $v_\theta = v_0$, where

$$v_\phi = R\dot{\phi}\cos\theta \tag{86}$$

$$v_\theta = R\dot{\theta} \tag{87}$$

are the eastward and northward velocity components [Eq. (25)]. Accordingly, Eqs. (82) and (83) give

$$\Omega\cos^2\theta_0 = \left(\Omega + \dot{\phi}\right)\cos^2\theta \tag{88}$$

$$\epsilon^2\Omega^2 = \dot{\phi}^2\cos^2\theta + \dot{\theta}^2, \tag{89}$$

where $\epsilon = v_0/\Omega R$ is the ratio of the puck's initial speed to the earth's tangential equatorial rotation speed.

Pucks with $\epsilon < \sin^2\theta_0$ never cross the equator. To see this, set $\theta = \dot{\theta} = 0$ in Eqs. (88) and (89), eliminate $\dot{\phi}$, and solve for ϵ.

$v_0 = 50$ m/s initial speed, $R = 6.37 \times 10^6$ m is the mean earth radius, $\Omega = 7.27 \times 10^{-5}$ s^{-1}, $\epsilon = 0.108$, and $\epsilon = \sin^2\theta_0$ gives $\theta_0 = 19°$.

For $\theta_0 = 30°$, the critical speed is $\mathbf{v}_0 = 116$ m/s.

Do $v_0 = 50$ m/s, $\theta_0 = 30°$, inertia circle frequency $\omega = 2\Omega\sin\theta_0 = 2\Omega\sin(30°) = \Omega$ same as earth's angular velocity. One inertia circle every 24 hours. Radius of the circle is $r_0 = v_0/\omega = 6.88 \times 10^5$ m which is 427 miles. Diameter of circle is 855 miles, from San Francisco to

Denver. Westward drift velocity is

$$v_\phi = -R\sin\theta_0\dot{\phi} \tag{90}$$
$$= -\epsilon^2 R\sin\theta_0\dot{\phi}_2 \tag{91}$$
$$= -\epsilon^2 R\sin\theta_0\frac{\Omega}{4\sin^2\theta_0} \tag{92}$$
$$= -\epsilon^2 R\frac{\Omega}{2} \tag{93}$$
$$= -2.7m/s \tag{94}$$

$R = 6.37\times10^6$ m is the mean earth radius, $\Omega = 7.27\times10^{-5}$ s^{-1}, $\epsilon = 0.108$. At 2.7 m/s, the drift is 2.3×10^5 m, or 145 miles, or 1/6 of the total diameter of the inertia circle.

To investigate small-amplitude motion in the vicinity of the puck's initial location (ϕ_0,θ_0), we expand ϕ and θ according to

$$\phi(t) = \phi_0 + \epsilon\phi_1 + \epsilon^2\phi_2 + \cdots \tag{95}$$
$$\theta(t) = \theta_0 + \epsilon\theta_1 + \epsilon^2\theta_2 + \cdots \tag{96}$$

We use the Taylor expansion

$$f(\theta) = f(\theta_0)+f'(\theta_0)(\theta-\theta_0)+\frac{1}{2}f''(\theta_0)(\theta-\theta_0)^2+\cdots \tag{97}$$

to expand $f(\theta)=\cos^2\theta$, yielding

$$\cos^2\theta = \cos^2\theta_0 - \epsilon\theta_1\sin2\theta_0 \tag{98}$$
$$-\epsilon^2\left(\theta_2\sin2\theta_0+\theta_1^2\cos2\theta_0\right)+\cdots. \tag{99}$$

To order ϵ, Eq. (88) yields

$$\dot{\phi}_1 = 2\Omega\theta_1\tan\theta_0. \tag{100}$$

To order ϵ^2, Eq. (89) yields

$$\Omega^2 = \dot{\phi}_1{}^2\cos^2\theta_0 + \dot{\theta}_1{}^2. \tag{101}$$

Inserting Eq. (99) into Eq. (100) gives

$$\Omega^2 = \omega^2\theta_1^2 + \dot{\theta}_1^2, \tag{102}$$

where

$$\omega = 2\Omega\sin\theta_0 \tag{103}$$

is an angular frequency. Separating variables, integrating, and applying the initial conditions gives

$$\theta_1(t) = \frac{\Omega}{\omega}\sin\omega t. \tag{104}$$

Inserting Eq. (103) into Eq. (99), integrating, and applying the initial conditions gives

$$\phi_1(t) = \frac{\Omega}{\omega\cos\theta_0}\left(1-\cos\omega t\right). \tag{105}$$

To order ϵ^2, Eq. (88) yields

$$\dot{\phi}_2 = 2\Omega\theta_2\tan\theta_0 + \Omega\left(\csc^2 2\theta_0 + \frac{1}{2}\sec^2\theta_0\right)\sin^2\omega t. \tag{106}$$

To order ϵ^3, Eq. (89) yields

$$\dot{\phi}_2\cos\theta_0\sin\omega t + \dot{\theta}_2\cos\omega t = \frac{\Omega^2}{\omega}\tan\theta_0\sin^3\omega t. \tag{107}$$

Inserting Eq. (105) into Eq. (106) gives

$$\dot{\theta}_2\cos\omega t + \omega\theta_2\sin\omega t = -\frac{\Omega\cos\theta_0}{\sin^2 2\theta_0}\sin^3\omega t. \tag{108}$$

Equation (107) is a first-order linear inhomogeneous differential equation with time-dependent coefficients. Its solution

$$\theta_2 = \theta_2^{\rm gen} + \theta_2^{\rm par} \tag{109}$$

is the sum of the general solution

$$\theta_2^{\rm gen} = B\cos\omega t \tag{110}$$

to the associated homogeneous problem (setting the right side of Eq. (107) to zero) and a particular solution

$$\theta_2^{\rm par} = A + C\cos2\omega t \tag{111}$$

that involves the second harmonic oscillations of frequency 2ω. Substituting Eq. (108) into Eq. (107) and imposing the initial conditions determines the coefficients A, B, and C:

$$\theta_2 = \frac{\Omega\cos\theta_0}{\omega\sin^2 2\theta_0}\left(-\frac{3}{2}+2\cos\omega t-\frac{1}{2}\cos2\omega t\right). \tag{112}$$

Finally, substituting this result into Eq. (106) and integrating gives

$$\phi_2 = -\frac{\Omega t}{4\sin^2\theta_0} + \frac{2\Omega}{\omega}\frac{\sin\omega t}{\sin^2 2\theta_0} - \frac{1+\sin^2\theta_0}{\sin^2 2\theta_0}\frac{\Omega}{2\omega}\sin2\omega t \tag{113}$$

Ripa gets this westward drift, but we get the full time-dependent solution as well.

Thus, to first order in the perturbations we obtain

$$\phi(t) = \phi_0 + \frac{v_0}{R\omega\cos\theta_0}\left(1-\cos\omega t\right) \tag{114}$$
$$\theta(t) = \theta_0 + \frac{v_0}{R\omega}\sin\omega t \tag{115}$$
$$v_\phi(t) = v_0\sin\omega t \tag{116}$$
$$v_\theta(t) = v_0\cos\omega t. \tag{117}$$

We investigate motion in the vicinity of the puck's initial location (ϕ_0,θ_0) by writing

$$\phi(t) = \phi_0 + \phi'(t) \tag{118}$$
$$\theta(t) = \theta_0 + \theta'(t), \tag{119}$$

with ϕ' and θ' describing small perturbations about this location. We use the first-order Taylor expansion

$$\cos^2\theta \approx \cos^2\theta_0 - 2\theta' \sin\theta_0 \cos\theta_0 \tag{120}$$

to write Eq. (88) to first order,

$$\dot{\phi}' = 2\Omega\theta' \tan\theta_0, \tag{121}$$

and to write Eq. (89) to second order,

$$\frac{v_0^2}{R^2} = \dot{\phi}'^{\,2}\cos^2\theta_0 + \dot{\theta}'^{\,2}. \tag{122}$$

Inserting Eq. (120) into Eq. (121) gives

$$\frac{d\theta'}{dt} = \pm\sqrt{\frac{v_0^2}{R^2} - 4\Omega^2\sin^2\theta_0\,\theta'^2}. \tag{123}$$

Separating variables, integrating, and applying the initial conditions gives

$$\theta'(t) = \frac{v_0}{R\omega}\sin\omega t, \tag{124}$$

where

$$\omega = 2\Omega\sin\theta_0 \tag{125}$$

is the angular frequency. Inserting Eq. (123) into Eq. (120) and integrating gives

$$\phi'(t) = \frac{v_0}{R\omega\cos\theta_0}\left(1-\cos\omega t\right). \tag{126}$$

Thus, to first order in the perturbations we obtain

$$\phi(t) = \phi_0 + \frac{v_0}{R\omega\cos\theta_0}\left(1-\cos\omega t\right) \tag{127}$$

$$\theta(t) = \theta_0 + \frac{v_0}{R\omega}\sin\omega t \tag{128}$$

$$v_\phi(t) = v_0\sin\omega t \tag{129}$$

$$v_\theta(t) = v_0\cos\omega t. \tag{130}$$

These solutions describe small-amplitude horizontal uniform circular motion with angular frequency $\omega = 2\Omega\sin\theta_0$, speed v_0, and radius $r_0 = v_0/|\omega|$, called "inertia circles" or "inertia oscillations." The derivation is valid for small-amplitude oscillations with $v_0 \ll R\Omega$ and $r_0 \ll R$, and the oscillations persist to large amplitudes, where they develop a westward drift. In contrast with motion on a spherical earth, for which objects execute uniform circular motion in great circles around the earth's center, objects undergoing inertia oscillations remain close to their initial latitudes [13, 30–32].

The motion is clockwise in the northern hemisphere, where $\omega > 0$, and counterclockwise in the southern hemisphere, where $\omega < 0$. The frequency ω equals zero at the equator, matches the earth's angular frequency Ω at $|\theta| = 30°$, and exceeds this frequency for $|\theta| > 30°$.

Setting $v_0 = 0$ in Eqs. (126)-(129) corresponds to releasing a hockey puck at rest at (ϕ_0, θ_0) in the rotating frame on an frictionless ellipsoidal earth. And these equations predict that the puck will remain at rest at that location, in contrast with a spherical earth, for which the puck slides off to the equator.

VII. SIMULATIONS

User inputs:

1. Initial longitude (degrees) ϕ_0
2. Initial latitude (degrees) θ_0
3. Initial eastward velocity (m/s) v_{ϕ_0}
4. Initial northward velocity (m/s) $v_{\theta 0}$
5. Choose spherical or ellipsoidal earth

In the code, convert ϕ_0 and θ_0 to radians, and use the numerical inputs above to determine the initial values $\dot{\phi}_0$ and $\dot{\theta}_0$ (measured in radians per second) from

$$v_{\phi_0} = R\cos\theta_0\dot{\phi}_0 \tag{131}$$

$$v_{\theta 0} = R\dot{\theta}_0, \tag{132}$$

where $R = 6.37\times10^6$ m is the mean earth radius and $\Omega = 7.27\times10^{-5}$ s^{-1} is the earth's angular velocity.

At this point, we have numerical values for ϕ_0 and θ_0 in radians, and $\dot{\phi}_0$ and $\dot{\theta}_0$ in radians per second. Knowing these, we can determine the constants of motion from [see Eqs. (69), (70), (82), and (83)]

$$L_0 = \left(\Omega + \dot{\phi}_0\right)\cos^2\theta_0 \text{ (spherical and ellipsoidal)} \tag{133}$$

$$T_0 = \left(\Omega + \dot{\phi}_0\right)^2\cos^2\theta_0 + \dot{\theta}_0^2 \text{ (spherical)} \tag{134}$$

$$T = \dot{\phi}_0^2\cos^2\theta_0 + \dot{\theta}_0^2 \text{ (ellipsoidal)}. \tag{135}$$

Knowing these constants of motion, use Euler integration or Runge-Kutta to integrate the equations of motion [derived from Eqs. (69), (70), (82), and (83)]

$$\dot{\phi} = \frac{L_0}{\cos^2\theta} - \Omega \text{ (spherical and ellipsoidal)} \tag{136}$$

$$\dot{\theta} = \pm\sqrt{T_0 - \frac{L_0^2}{\cos^2\theta}} \text{ (spherical)} \tag{137}$$

$$\dot{\theta} = \pm\sqrt{T - \frac{\left(L_0 - \Omega\cos^2\theta\right)^2}{\cos^2\theta}} \text{ (ellipsoidal)} \tag{138}$$

You need two equations of motion (the first two) to do motion on the spherical earth, and two equations of motion (the first and the third) to do motion on the ellipsoidal earth.

*** the rest of this paper is rough ***

The longitude ϕ' is the angle measured eastward from the prime meridian, and is used in conjunction with the latitude θ to specify geographical locations on the earth's surface.

For motion on the rotating earth, the "fixed" frame is the inertial frame of reference of a stationary observer in space, looking down on the rotating earth (Fig. 1a), and the "rotating" frame is the non-inertial frame of reference of an earthbound observer who co-rotates with the

earth (Fig. 1b). The fixed-frame coordinates (x, y, z) are stationary with respect to the stars, whereas the rotating-frame coordinates (x', y', z') rotate with the earth at its angular velocity $\mathbf{\Omega} = \Omega\hat{z}$ $(z = z')$, and puncture the earth's surface at specific geographical locations.

In the fixed frame (Fig. 1a), the position vector $\mathbf{r}$ of an object on the surface is specified by an azimuthal angle ϕ, latitude θ, and distance $r = R(\theta)$ from the earth's center (Fig. 7). In the rotating frame (Fig. 1b), the position vector $\mathbf{r}$ is specified by a longitude

$$\phi' = \phi - \Omega t, \tag{139}$$

latitude θ, and distance $r = R(\theta)$ from the earth's center. The latitude and longitude are used to specify geographical locations on the earth's surface.

Objects that are constrained to move on the surface of the earth have two horizontal components of velocity, an eastward component and a northward component. In the fixed frame (Fig. 1a), we denote the horizontal velocity vector as $\mathbf{v}$, and its eastward and northward components as $v_\mathrm{e} = \rho(\theta)\dot{\phi}$ and v_n. In the rotating frame (Fig. 1b), we denote the horizontal velocity vector as $\mathbf{v}'$, and its eastward and northward components as $v'_\mathrm{e} = \rho(\theta)\dot{\phi}'$ and v_n, noting that the northward components are the same in the two frames. Combining these definitions with Eq. (**??**) and the time derivative of Eq. (138) yields a relationship between the eastward components of velocity,

$$v'_\mathrm{e} = v_\mathrm{e} - V(\theta). \tag{140}$$

This relationship emphasizes the essential difference between the velocity vectors in the two frames. The enormous tangential speed of rotation of the earth $V(\theta)$ is included in the eastward velocity v_e seen by an observer in the fixed frame, whereas the eastward velocity v'_e seen by an observer in the rotating frame includes only motion relative to an earthbound observer who co-rotates with the earth.

*****

A. Fundamental concepts

Four principles are needed to address and correct Hadley's principle. These principles apply to drag-free projectile motion of an object above the earth's surface, and also apply to the motion of an object sliding without friction on a spherical or ellipsoidal earth. These principles exploit the pedagogical simplicity of conservation laws in the inertial frame in order to explain the mysterious motions in the rotating frame [15, 67], and take the point of view of an inertial observer:

Fundamental concepts:

1. *The earth's eastward rotation speed depends on latitude.* As seen by an observer in the fixed frame, all points on the earth's surface complete one rotation about the earth's rotation axis each day, moving toward the east. Points on the earth's equator are farthest from this axis and travel the farthest each day, so these points travel the fastest of all points on the earth's surface, at about 460 m/s. This rotation speed decreases as one moves from the equator to one of the poles, where the rotation speed is zero.
2. *The velocity vector of an object depends on the reference frame from which it is viewed.* An object that travels due north as seen by an observer in the rotating frame travels northeast as seen by an observer in the fixed frame.
3. *The local compass directions (north, east, and up) depend on one's position on the earth's surface (Fig.* **??***).* As seen by an observer in the fixed frame, the local compass directions point in different directions at different points on the earth. For example, the "up" direction at the north pole is directed opposite to the "up" direction at the south pole.
4. *Energy is conserved.* As seen by an observer in the fixed frame, the object's total mechanical energy (the sum of its kinetic and gravitational potential energies) is conserved.
5. *Angular momentum is conserved.* As seen by an observer in the fixed frame, earth's gravity increases the eastward velocity of objects as they move closer to the earth's rotation axis, and decreases this velocity as they move away (Fig. **??**).

math ahead The earth's eastward rotation speed V is given by $V = \Omega R\cos\phi$, where Ω is the magnitude of the earth's angular velocity, R is the earth's radius, and ϕ is the latitude (Fig. **??**). V is at maximum at the equator ($\phi = 0$) and is zero at the poles ($\phi = \pm\pi/2$).

objects move closer to the earth's axis of rotation, the earth's gthey speedObjects speed up as they move closer to the earth's axis of rotation, and slow down as they move away. This is because the force to conserve angular momentum. that move closer to the axis of rotation speedAs seen by an observer in the fixed frame, an object that the object's axial angular momentum $l_z = mv_\mathrm{e}\rho$ is conserved, where v_e is the object's eastward component of velocity and $\rho = r\cos\phi$ is the distance of the object from the earth's rotation axis [31, 64]

Here are Ben's references: [23, 68–70]

Misconceptions:

1. *No eastward component of velocity*
2. *No concept of rotating frame*
3. *No differential rotation*
4. *Eastward component of velocity constant*
5. *East ain't always east (curvilinear geometry)*

Hadley's principle predicts the correct direction of the Coriolis deflection, but accounts for only half of its magnitude. Invoking conservation of angular momentum

(Principle 4) accounts for the other half: As the object moves northward on the earth's surface, its eastward component of velocity $v_{\rm e}$ must *increase* as its distance ρ from the earth's rotation axis decreases in order to keep $l_z = mv_{\rm e}\rho$ constant, thereby accounting for the missing deflection [3].

We can also make a geometrical argument for this increase in $v_{\rm e}$, an argument that incorporates the curvilinear compass directions (Principle 2). Figure **??** shows a great circle around a spherical earth, the path taken by an object that slides without friction along its surface. Shown are velocity vectors $\mathbf{v}$ and their eastward and northward components, $v_{\rm e}$ and $v_{\rm n}$. These components are equal where the great circle intersects the equator, whereas $v_{\rm n} = 0$ where the great circle draws tangent to the 45° latitude line, and where all of the particle's momentum is toward the east. To offset the decrease in $v_{\rm n}$ as the object moves northward, $v_{\rm e}$ must increase to ensure constant speed,

$$v = \sqrt{v_{\rm e}^2 + v_{\rm n}^2}. \tag{141}$$

Without this increase in $v_{\rm e}$, the speed cannot remain constant and mechanical energy cannot be conserved (Principle 3). As seen by an observer in the rotating frame, the Coriolis force is solely responsible for the increase in $v_{\rm e}$, and the centrifugal and Coriolis forces conspire to decrease $v_{\rm n}$.

In summary, Hadley's principle obeys Principle 1 and violates Principles 2, 3, and 4. All four principles are needed to fully understand the Coriolis deflection, and will serve as the basis for our lecture videos (Sec. **??**). Hadley's principle hurts more than it helps in developing understanding of the physical origins of the Coriolis force, yet it continues to be used widely in textbooks to explain these origins. Our dissemination plan includes efforts to encourage authors to replace such explanations with more complete ones (Sec. **??**).

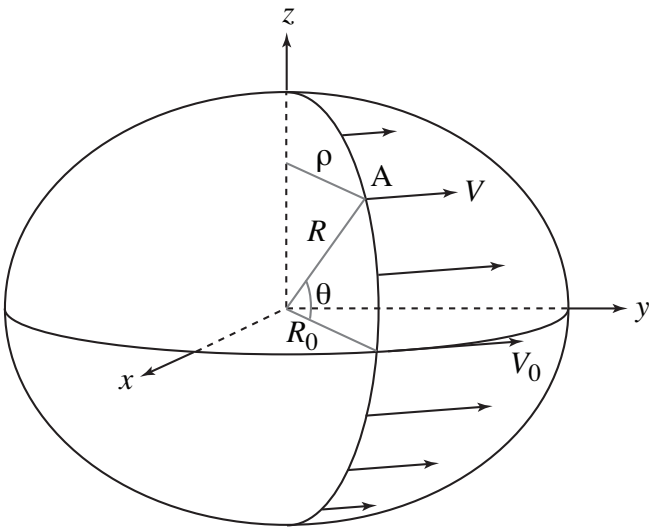

FIG. 7. Diagram showing the latitude dependence of the radius $R(\theta)$, axis distance $\rho(\theta)$, and eastward tangential rotation speed $V(\theta)$ at a point A on the surface of a rigid ellipsoidal earth, as seen by an observer that is fixed in space, looking down on the rotating earth. Newton's second law applies in this "fixed" inertial reference frame, in which the coordinates (x, y, z) are fixed with respect to the stars [Eq. (1)]. Here, R_0 and V_0 are the radius and rotation speed at the equator. In this and subsequent figures, the non-sphericity of the earth is exaggerated.

[1] A. Persson, History of Meteorology **2**, 1 (2005).
[2] G. G. Coriolis, J. Ecole Polytech. **15**, 142 (1835).
[3] A. Persson, Bulletin of the American Meteorological Society **79**, 1373 (1998).
[4] P. A. Tyvand and K. B. Haugen, Physics of Fluids **17**, 062105 (2005).
[5] M. S. Tiersten and H. Soodak, American Journal of Physics **68**, 129 (2000).
[6] A. Shakur, The Physics Teacher **52**, 464 (2014).
[7] A. O. Persson, History of Meteorology **3**, 17 (2006).
[8] M. S. Tiersten and H. Soodak, American Journal of Physics **66**, 810 (1998).
[9] J. Tessman, American Journal of Physics **55**, 392 (1987).
[10] J. A. Van den Akker, American Journal of Physics **55**, 1063 (1987).
[11] National Geographic, "Coriolis Effect Demonstration," `https://youtu.be/mPsLanVS1Q8` (accessed 21-Nov-2018) (2018).
[12] A. Persson, Meteorological Applications **17**, 236 (2010).
[13] A. Persson, Quarterly Journal of the Royal Meteorological Society **141**, 1957 (2015).
[14] J. R. Taylor, *Classical mechanics* (University Science Books, 2005).
[15] D. H. McIntyre, American Journal of Physics **68**, 1097 (2000).
[16] J. M. Moran, *Weather studies: Introduction to atmospheric science*, 5th ed. (American Meteorological Society, Boston, Massachusetts, 2012).
[17] D. Thomas and D. G. Bowers, *Introducing Oceanography* (Dunedin Academic Press Ltd, 2012).
[18] National Geographic, "Coriolis Effect," `https://www.nationalgeographic.org/encyclopedia/coriolis-effect/` (accessed 21-Nov-2018) (2018).
[19] G. Hadley, Phil. Trans. Roy. Soc. London **39**, 58 (1735).
[20] C. Abbe, *The Mechanics of the Earth's Atmosphere: A Collection of Translations*, Vol. 51 (contains a translation of Hadley's 1735 article) (Smithsonian institution, 1910).
[21] J. Renault and E. Okal, American Journal of Physics **45**, 631 (1977).
[22] L. J. Battan, *Fundamentals of meteorology*, 2nd ed. (Englewood Cliffs: Prentice-Hall, 1984).
[23] B. J. Skinner, S. C. Porter, and J. Park, *Dynamic earth:*

an introduction to physical geology, 5th ed. (John Wiley & Sons, 2004).
[24] D. Stirling, American Journal of Physics **51**, 236 (1983).
[25] E. Reddingius, American Journal of Physics **52**, 562 (1984).
[26] D. Stirling, American Journal of Physics **52**, 563 (1984).
[27] R. Bauman, The Physics Teacher **21**, 461 (1983).
[28] J. Boyd and P. Raychowdhury, American Journal of Physics **49**, 498 (1981).
[29] P. Mohazzabi, American Journal of Physics **67**, 1017 (1999).
[30] D. R. Durran, Bulletin of the American Meteorological Society **74**, 2179 (1993).
[31] P. Ripa, Journal of Physical Oceanography **27**, 633 (1997).
[32] J. R. Holton and G. J. Hakim, *An Introduction to Dynamic Meteorology*, Vol. 88 (Academic Press, 2013).
[33] A. L. Fetter and J. D. Walecka, *Theoretical mechanics of particles and continua*, first edition ed. (McGraw-Hill, 1980).
[34] A. Persson, "Private communication with B. Edwards," (2018).
[35] P. B. Kohl, D. Rosengrant, and N. D. Finkelstein, Physical Review Special Topics-Physics Education Research **3**, 010108 (2007).
[36] N. S. Podolefsky and N. D. Finkelstein, Physical Review Special Topics-Physics Education Research **3**, 020104 (2007).
[37] N. S. Podolefsky and N. D. Finkelstein, Physical Review Special Topics-Physics Education Research **3**, 010109 (2007).
[38] N. S. Podolefsky and N. D. Finkelstein, Physical Review Special Topics-Physics Education Research **2**, 020101 (2006).
[39] C. Baily and N. D. Finkelstein, Physical Review Special Topics-Physics Education Research **11**, 020124 (2015).
[40] D. H. McIntyre, "Coriolis force and noninertial effects animations," `http://physics.oregonstate.edu/~mcintyre/coriolis` (accessed 20-Nov-2018) (2018).
[41] M. Littell, "Observe an animation of the Coriolis effect over Earth's surface," `http://www.classzone.com/books/earth_science/terc/content/visualizations/es1904/es1904page01.cfm` (accessed 20-Nov-2018) (2018).
[42] NOAA, "Coriolis Effect," `http://noaacontent.nroc.org/lesson08/l8ex1.htm` (accessed 20-Nov-2018) (2018).
[43] C. Teunissen, "Coriolis effect," `http://www.cleonis.nl/physics/graphlets/coriolis_effect.php` (accessed 20-Nov-2018) (2018).
[44] udiprod, "Visualization of the Coriolis and centrifugal forces," `https://www.youtube.com/watch?v=49JwbrXcPjc` (accessed 20-Nov-2018) (2018).
[45] N. D. Finkelstein, W. K. Adams, C. Keller, P. B. Kohl, K. K. Perkins, N. S. Podolefsky, S. Reid, and R. LeMaster, Physical Review Special Topics-Physics Education Research **1**, 010103 (2005).
[46] N. Finkelstein, W. Adams, C. Keller, K. Perkins, C. Wieman, *et al.*, Journal of Online Learning and Teaching **2**, 110 (2006).
[47] K. Perkins, W. Adams, M. Dubson, N. Finkelstein, S. Reid, C. Wieman, and R. LeMaster, The Physics Teacher **44**, 18 (2006).
[48] C. E. Wieman, W. K. Adams, P. Loeblein, and K. K. Perkins, The Physics Teacher **48**, 225 (2010).
[49] C. E. Wieman, W. K. Adams, and K. K. Perkins, Science **322**, 682 (2008).
[50] W. K. Adams, S. Reid, R. LeMaster, S. B. McKagan, K. K. Perkins, M. Dubson, and C. E. Wieman, Journal of Interactive Learning Research **19**, 397 (2008).
[51] W. K. Adams, S. Reid, R. LeMaster, S. McKagan, K. Perkins, M. Dubson, and C. E. Wieman, Journal of Interactive Learning Research **19**, 551 (2008).
[52] S. McKagan, K. Perkins, and C. Wieman, Physical Review Special Topics-Physics Education Research **4**, 020103 (2008).
[53] R. J. Beichner, American Journal of Physics **64**, 1272 (1996).
[54] W. Christian and M. Belloni, *Physlets* (Prentice Hall Upper Saddle River, NJ, 2000).
[55] J. Bransford, S. Brophy, and S. Williams, Journal of Applied Developmental Psychology **21**, 59 (2000).
[56] B. F. Edwards and J. M. Edwards, Chaos: An Interdisciplinary Journal of Nonlinear Science **27**, 053107 (2017).
[57] three.js, "three.js," `https://threejs.org` (accessed 20-Nov-2018) (2018).
[58] D3, "D3," `https://d3js.org` (accessed 20-Nov-2018) (2018).
[59] JSXGraph, "JSXGraph," `https://jsxgraph.org/wp/index.html` (accessed 20-Nov-2018) (2018).
[60] Babylon.js, "Babylon.js," `https://www.babylonjs.com` (accessed 20-Nov-2018) (2018).
[61] CopperLicht, "CopperLicht," `https://www.ambiera.com/copperlicht` (accessed 20-Nov-2018) (2018).
[62] Phoria.js, "Phoria.js," `http://www.kevs3d.co.uk/dev/phoria/` (accessed 20-Nov-2018) (2018).
[63] K. Schwaber and M. Beedle, *Agile software development with Scrum*, Vol. 1 (Prentice Hall Upper Saddle River, 2002).
[64] J. J. Early, Quarterly Journal of the Royal Meteorological Society **138**, 1914 (2012).
[65] R. Stacey and P. Davis, *Physics of the Earth* (Cambridge University Press, 2008).
[66] Wikipedia, "Spherical trigonometry," `https://en.wikipedia.org/wiki/Spherical_trigonometry` (accessed 12-Dec-2018) (2018).
[67] J. F. Wild, American Journal of Physics **41**, 1057 (1973).
[68] J. Brown, A. Colling, D. Park, J. Phillips, D. Rothery, and J. Wright, *Ocean circulation: prepared by an Open University course team* (Pergamon Press, 1989) p. 238.
[69] J. Shipman, J. Wilson, and C. Higgins, *An introduction to physical science* (Nelson Education, 2012).
[70] B. J. Skinner and B. Murck, *The blue planet: an introduction to earth system science* (John Wiley & Sons, 2011).